Generalized complex inductance for radiation problems

Lap K. Yeung and **Ke-Li Wu**
Department of Electronic Engineering,
The Chinese University of Hong Kong, Shatin, NT, Hong Kong,
e-mail: lkyeung@ee.cuhk.edu.hk

Abstract

The concept of generalized complex inductance for the partial element equivalent circuit (PEEC) technique is introduced to model microstrip radiation problems. Using the semi-analytical Greens functions for microstrip substrates, the imaginary part of this generalized complex inductance can be shown to represent a frequency-dependent resistance containing information about the losses from spatial radiations (spherical and lateral) and surface waves (cylindrical). Hence, different radiation components can be derived separately, providing a useful and unique feature for representing high-speed/high frequency microstrip structures and antennas in the network domain.

1 Introduction

Although the partial element equivalent circuit (PEEC) technique [1–3] has been successfully applied for analyzing a wide range of electromagnetic problems, including electromagnetic compatibility, electromagnetic interference, as well as signal integrity for high-speed electronic circuits, its ability to handle radiation problems has not been considered thoroughly. Recently, a radiation model for the PEEC technique has been proposed for the free-space case [4]. This model makes use of the concept of generalized complex inductance to account for the radiation effect and the corresponding PEEC model can be used as a starting point to extract essential information on the radiation characteristics of the structure being investigated. In this work, the radiation model is extended to the case of modeling microstrip circuits and antennas. By using the Green's functions for microstrip substrates, it can

Pulsed Electromagnetic Fields: Their Potentialities, Computation and Evaluation
I. E. Lager and L. J. Jiang (Eds.).
doi: 10.3233/978-1-61499-230-1-65

be shown that the imaginary part of the inductance represents a frequency-dependent resistance containing contributions from spatial radiation and surface waves. The resulting equivalent circuits employing this generalized complex inductance concept require no 'non-conservative' capacitors, and the (quasi-)static condition for the capacitive components is preserved.

2 Theory

2.1 Single-layered microstrip Greens functions

Magnetic vector and electric scalar Greens functions for microstrip structures are usually expressed in terms of Sommerfeld integral as

$$G = \int \tilde{G}\left(k_\rho\right) H_0^{(2)}\left(k_\rho \rho\right) k_\rho \mathrm{d}k_\rho \tag{1}$$

where $\tilde{G} = \tilde{G}_A^{xx}$ or $\tilde{G}_\phi$ is the corresponding Greens function in the spectral domain, and $H_0^{(2)}$ is the Hankel function of the second kind. In order to compute this integral, a variety of techniques can be used. In general, for a single-layered microstrip substrate, the two spectral-domain Greens functions can be decomposed into three parts [5] as

$$\tilde{G} = \tilde{G}_0 + \tilde{G}_{\mathrm{SW}} + \frac{F}{\mathrm{j}2k_{z0}}. \tag{2}$$

Notice that $k_{z0}^2 = k_0^2 - k_\rho^2$. The first two terms in (2) represent, respectively, the asymptotic ($k_\rho \to \infty$) and surface-wave components of the Greens function. The last term F is the 'leftover' for which the first two components do not cover.

In this work, the asymptotic and the 'leftover' components are considered together as they both contribute to radiation into free space. In this sense, Eq. (2) should be rewritten as

$$\tilde{G} = \left(\tilde{G}_0 + \frac{F}{\mathrm{j}2k_{z0}}\right) + \tilde{G}_{\mathrm{SW}} = \tilde{G}_{\mathrm{SP}} + \tilde{G}_{\mathrm{SW}} \tag{3}$$

The corresponding spatial domain Greens functions can be obtained through (1).

2.2 Generalized complex inductance

The 'non-conservative' capacitance issue can be overcome by extracting only the (quasi-)static portion of the electric scalar Greens function for

calculating the shorted-circuit capacitance matrix and moving its frequency-dependent portion to the inductance matrix. It is, mathematically, done by separating $G_{\phi,\mathrm{SP}}$ into two parts as

$$G^0_{\phi,\mathrm{SP}} = G_{\phi,\mathrm{SP}} \quad \text{with } k_0 \to 0 \tag{4}$$

$$G^{\mathrm{f}}_{\phi,\mathrm{SP}} = G_{\phi,\mathrm{SP}} - G^0_{\phi,\mathrm{SP}}. \tag{5}$$

This treatment then leads to the coefficient of potential as

$$pp_{i,n} = pp^0_{i,n} + pp^{\mathrm{f}}_{i,n} = \frac{1}{a_i a_n} \iint G^0_{\phi,\mathrm{SP}} \,\mathrm{d}s'_n \mathrm{d}s_i + \frac{1}{a_i a_n} \iint \left(G^{\mathrm{f}}_{\phi,\mathrm{SP}} + G_{\phi,\mathrm{SP}} \right) \mathrm{d}s'_n \mathrm{d}s_i \tag{6}$$

between capacitive mesh i and mesh n. The frequency-dependent second integral is used only for generating the inductive matrix.

The mutual inductance between two inductive meshes (l and m) or self-inductance ($l = m$) is given by

$$L_{l,m} = \frac{1}{w_l w_m} \iint \left(G^{xx}_{\mathrm{A,SP}} + G^{xx}_{\mathrm{A,SW}} \right) \mathrm{d}s'_n \mathrm{d}s_i. \tag{7}$$

It is generally a complex number. As there is no matrix inversion involved here, the imaginary part does produce a physically meaningful self-resistance ($l = m$). Now, by absorbing the second integral in (6) into the inductance term (7), a generalized self- and mutual inductance is formed. The resulting generalized inductance becomes (see Fig. 1)

$$\bar{L}_{l,m} = L_{l,m} + \frac{pp^{\mathrm{f}+}_{l,n_1}}{\omega^2} - \frac{pp^{\mathrm{f}-}_{l,n_1}}{\omega^2} - \frac{pp^{\mathrm{f}+}_{l,n_2}}{\omega^2} + \frac{pp^{\mathrm{f}-}_{l,n_2}}{\omega^2}. \tag{8}$$

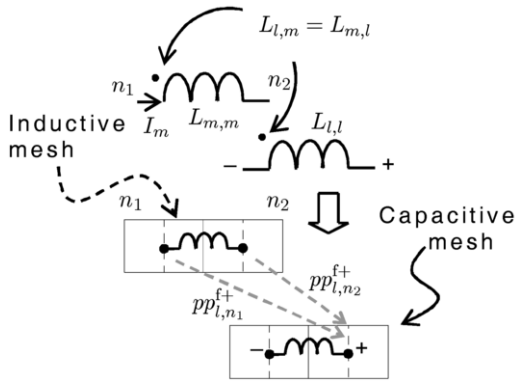

Figure 1: Coupling configuration between inductors l and m.

The significance of introducing such generalized inductance is that it not only correctly accounts for the radiation effect, but also preserves the physical meaning of the capacitance matrix.

3 Results

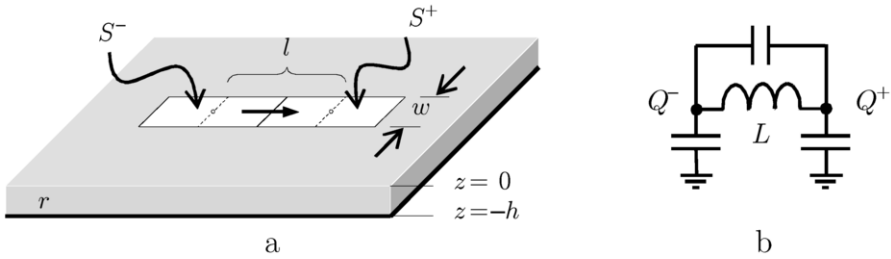

Figure 2: Short dipole on microstrip substrate. (a) Physical configuration; (b) equivalent circuit.

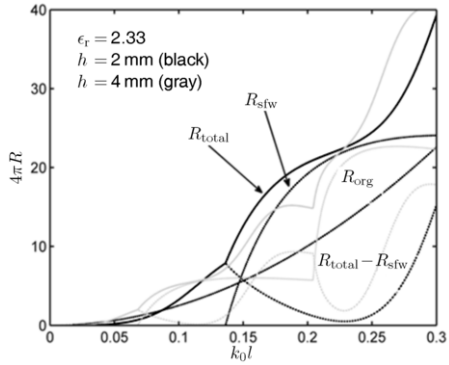

Figure 3: Radiation resistance components of a short dipole on microstrip substrate for $h = 2\,\mathrm{mm}$ and $h = 4\,\mathrm{mm}$.

3.1 Short dipole on microstrip substrate

Following the discussion above, the real part of the term $\mathrm{j}\omega L$ (radiation resistance) of an short (infinitesimal) dipole on microstrip substrate (see Fig. 2) can be decomposed into four components including the original free-space term, the term due to quasi-static images, the surface-wave term, and the remaining term contributed by lateral waves and other higher order effects. Fig. 3 depicts the cases of $\epsilon_\mathrm{r} = 2.33$, $h = 2\,\mathrm{mm}$ and $h = 4\,\mathrm{mm}$. It can be seen from the figure that, for the $h = 2\,\mathrm{mm}$ case, the surface

waves do not radiate ($R_{\text{sfw}} = 0$) until $k_0 l$ reaches ∼0.13. At this point, the component ($R_{\text{total}} - R_{\text{sfw}}$) represents the power radiated into free-space drops significantly. A similar feature can be seen for the $h = 4\,\text{mm}$ case. In this case, the power radiated into free-space drops every time when a new surface wave mode starts propagating.

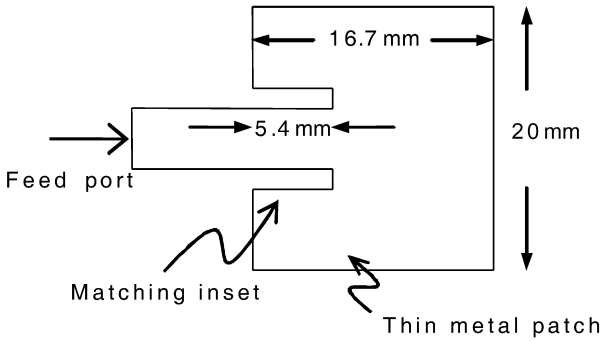

Figure 4: Geometry for the patch antenna.

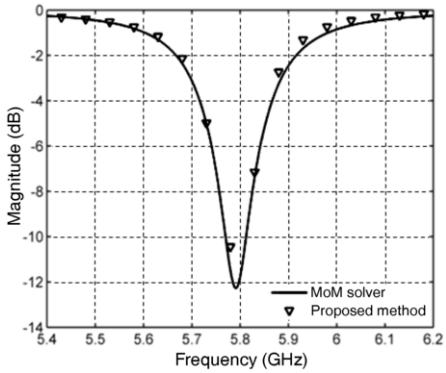

Figure 5: Simulated results ($|S_{11}|$) for the patch antenna with negligible surface waves.

3.2 Patch antenna

Another example to be studied is a patch antenna on thin substrate. The substrate used in this example has a dielectric constant of 2.33 and a thickness of 0.787 mm. As the substrate is thin and has a small value of dielectric constant, the surface wave contributions to the Greens functions are relatively insignificant at low frequencies. The size of the patch antenna (see Fig. 4) is 16.7 mm × 20 mm. It is fed by a microstrip with an inset of 5.4 mm to match to a 50 Ω transmission line. The geometry is divided into a

total of 127 capacitive meshes and 222 inductive meshes, corresponding to a meshing scheme of ∼30 meshes per (free-space) wavelength at 6.2 GHz. From the simulated results in Fig. 5, it is seen that the patch operates at around 5.8 GHz. The scattering parameters calculated by the PEEC technique using the concept of generalized complex inductance agree well with those from a MoM-based commercial EM solver.

4 Model reduction

Generally, it is not easy to obtain any physical insights by directly examining a PEEC-generated equivalent circuit. To obtain a more concise and physically intuitive circuit model, the model order reduction (MOR) technique described in [6] can be used. In this technique, most circuit nodes except the port nodes (nodes connecting to the source) of a PEEC-generated equivalent circuit are eliminated by using the $Y-$ to $-\Delta$ transformation. Following a set of elimination criteria, the circuit can usually be simplified to containing only a few nodes. For the example shown in Fig. 6, if the dipole is electrically small, its equivalent circuit may be reduced to a pure capacitive circuit with only three capacitors (Fig. 7). It is important to notice that the inductive components get mixed with the capacitive components and vice versa during the reduction process and this leads to the final simplified circuit containing complex-valued capacitors as well.

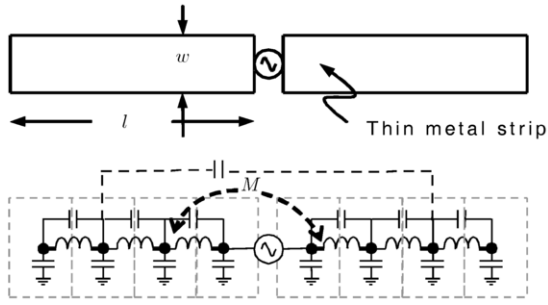

Figure 6: Short thin-strip dipole and its PEEC model.

An antenna is considered to be electrically small if it satisfies the inequality of $ka \leqslant 0.5$, where k is the free-space propagation constant and a is the radius of the smallest sphere that can completely encloses the antenna. Two short thin-strip dipoles, namely, a straight dipole and a meandered dipole (Fig. 8) are investigated here with $ka = 0.5$ at 4 GHz. Assuming there is no conductor loss, it is expected that the meandered dipole should have a smaller radiation quality (Q) factor when comparing to the straight

Table 1: Component values for the straight dipole.

f (GHz)	C_1 (F)	C_2 (F)
1	$1.41 \times 10^{-14} - \mathrm{j}3.04 \times 10^{-18}$	$7.30 \times 10^{-14} - \mathrm{j}2.23 \times 10^{-21}$
2	$1.44 \times 10^{-14} - \mathrm{j}2.52 \times 10^{-17}$	$7.35 \times 10^{-14} - \mathrm{j}7.31 \times 10^{-20}$
3	$1.49 \times 10^{-14} - \mathrm{j}8.98 \times 10^{-17}$	$7.45 \times 10^{-14} - \mathrm{j}5.76 \times 10^{-19}$
4	$1.57 \times 10^{-14} - \mathrm{j}2.31 \times 10^{-16}$	$7.58 \times 10^{-14} - \mathrm{j}2.57 \times 10^{-18}$

Table 2: Component values for the meandered dipole

f (GHz)	C_1 (F)	C_2 (F)
1	$4.50 \times 10^{-14} - \mathrm{j}1.95 \times 10^{-17}$	$1.37 \times 10^{-13} - \mathrm{j}7.79 \times 10^{-21}$
2	$5.09 \times 10^{-14} - \mathrm{j}1.91 \times 10^{-16}$	$1.44 \times 10^{-13} - \mathrm{j}2.97 \times 10^{-19}$
3	$6.53 \times 10^{-14} - \mathrm{j}9.76 \times 10^{-16}$	$1.59 \times 10^{-13} - \mathrm{j}3.12 \times 10^{-18}$
4	$1.08 \times 10^{-13} - \mathrm{j}5.26 \times 10^{-15}$	$1.92 \times 10^{-13} - \mathrm{j}2.37 \times 10^{-17}$

one. However this information cannot be seen by simply looking at their PEEC models. On the other hand, this can be easily confirmed from the concise circuit models derived by the algorithm discussed above. In both cases, their PEEC-generated equivalent circuits can be simplified to the one shown in Fig. 7 with the corresponding components values listed in Table 1 and Table 2, respectively.

By looking at the concise circuit models for these two antennas, it is clear that they are both electric-type within the operating frequency band of interest (<4 GHz) because they can be modeled by a circuit with only capacitors. Another interesting fact is that these complex-valued capacitors have their imaginary values increase with the operating frequency. In fact, the imaginary part of such a capacitor represents its loss from radiation. When looking into the excitation port, the circuit in Fig. 7 can be further

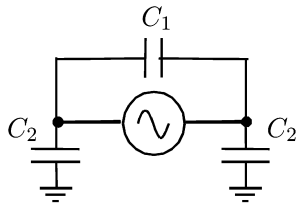

Figure 7: Short thin-strip dipole and its PEEC model.

simplified to just a single capacitor of value $C = C_1 + C_2/2$. Its quality factor is approximately the radiation Q factor of the antenna. Fig. 9 shows the excitation port admittance and the approximated Q factors for the two antennas at different operating frequencies. It can be seen from the figure that the radiation resistance (conductance) of the meandered dipole increases rapidly when ka approaching 0.5. To verify the accuracy of our simplified circuit models, results (solid lines) obtained from a commercial full-wave electromagnetic solver are also shown and they agree well with each other.

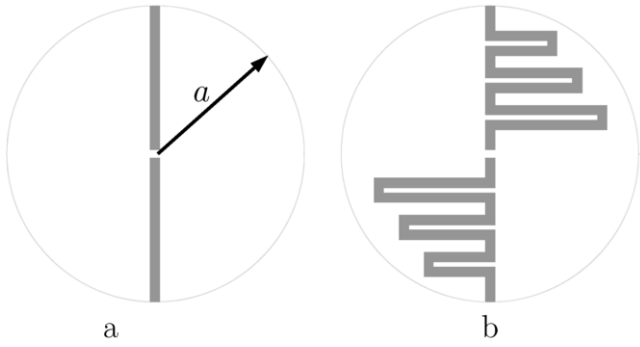

Figure 8: Straight (a) and meandered (b) small dipoles.

5 Conclusions

A new PEEC formulation, which incorporates the concept of generalized complex inductance, for modeling of microstrip structures has been introduced. In this PEEC formulation, the radiation loss is taken into account by having complex-valued inductors in the equivalent circuit. And through these inductors, contributions from various radiation mechanisms, such as spatial and surface waves, to the overall radiation are revealed. In addition, a technique to automatically derive a concise and physically intuitive equivalent circuit model for an electrically small radiating structure is presented. Important information such as radiation resistance, capacitive and inductive storage energy of the structure can be identified directly by examining this concise circuit model. In addition, such a circuit model can readily be incorporated into other higher level design exercises so that impacts of the structure on the overall system performance can easily be simulated. The proposed algorithm is, therefore, useful for modern integrated high-speed/high-frequency circuit design.

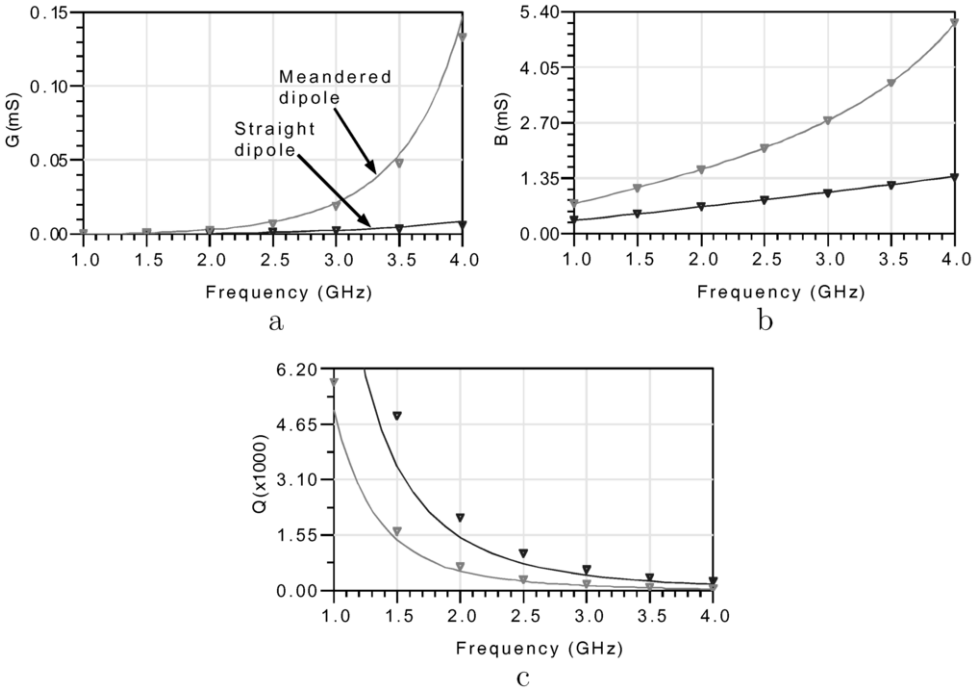

Figure 9: Simulated port for the two example dipoles. (a) Conductance; (b) susceptance; (c) approximated radiation Q factors.

Acknowledgment

The authors wish to acknowledge the supports from University Grants Committee of Hong Kong under Grant AoE/P-04/08 and Innovation Technology Commission of Hong Kong under Grant ITS/019/10.

Bibliography

[1] A. Ruehli, "Equivalent circuit models for three dimensional multiconductor systems," *IEEE Trans. Microwave Theory Tech.*, vol. 22, no. 3, pp. 216–221, March 1974.

[2] H. Heeb and A. Ruehli, "Three-dimensional interconnect analysis using partial element equivalent circuits," *IEEE Trans. Circuits and Systems*, vol. 39, no. 11, pp. 974–982, Nov. 1992.

[3] A. Ruehli, "Circuit models for three-dimensional geometries including dielectrics," *IEEE Trans. Microwave Theory Tech.*, vol. 40, no. 7, pp. 1507–1516, July 1992.

[4] L. K. Yeung and K.-L. Wu, "Generalized partial element equivalent circuit (PEEC) modeling with radiation effect," *IEEE Trans. Microwave Theory Tech.*, vol. 59, no. 10, pp. 2377–2384, Oct. 2011.

[5] Y. Chow, J. Yang, D. Fang, and G. Howard, "A closed-form spatial Greens function for the thick microstrip substrate," *IEEE Trans. Microwave Theory Tech.*, vol. 39, no. 3, pp. 588–592, July 1991.

[6] J. Wang and K.-L. Wu, "A derived physically expressive circuit model for multilayer RF embedded passives," *IEEE Trans. Microwave Theory Tech.*, vol. 54, no. 5, pp. 1961–1968, May 2006.